


MODULATION OF NICOTINIC RECEPTORS BY AN ALLOSTERIC LIGAND ASSESSED
USING FAST JUMPS IN ACETYLCHOLINE


By

Spencer L. Hirt

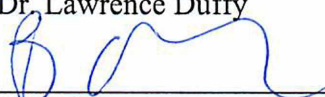
RECOMMENDED:




Dr. Kelly Drew



Dr. Lawrence Duffy




Dr. Brian Edmonds
Advisory Committee Chair

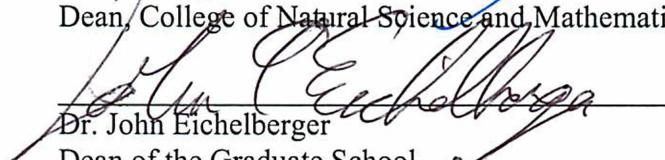


Dr. Thomas Green
Chair, Department of Chemistry and Biochemistry

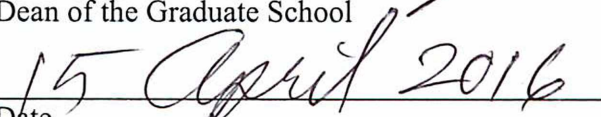
APPROVED:



Dr. Paul Lauer
Dean, College of Natural Science and Mathematics



Dr. John Eichelberger
Dean of the Graduate School



Date 15 April 2016

MODULATION OF NICOTINIC RECEPTORS BY AN ALLOSTERIC LIGAND ASSESSED
USING FAST JUMPS IN ACETYLCHOLINE

A

Thesis

Presented to the Faculty
of the University of Alaska Fairbanks
in Partial Fulfillment of the Requirements
for the Degree of

MASTER OF SCIENCE

By

Spencer L. Hirt, B.A.

Fairbanks, AK

May 2016

Abstract

Properties of ligand-gated ion channels such as $\alpha 4\beta 2$ nicotinic acetylcholine receptors (nAChRs) and their interactions with various pharmacologic compounds have been studied using voltage clamping techniques for decades. The peak current amplitude, measured in whole-cell experiments, gives us an idea of how receptors will respond to a ligand *in situ*. Some ligands have the potential to potentiate the peak amplitude, by various mechanisms such as destabilization of receptor desensitized states. The ability of a ligand to increase the peak amplitude of $\alpha 4\beta 2$ nAChRs has the potential to treat a variety of neuronal disorders; however unique properties of these receptors such as fast activation and long-lived desensitized states create significant challenges in determining the extent of modulation of the peak current using these techniques. To correctly assess the peak amplitude, the experiment must achieve synchronous activation of all surface receptors by optimizing solution exchange rates. Failure to do so leads to blunted peak-amplitude measurements in acetylcholine (ACh).

This study found that previous reports of the modulating effects of desformylflustrabromine (dFBr), a positive allosteric modulator (PAM) of $\alpha 4\beta 2$ nAChRs, neglected to account for the large surface area of *Xenopus* oocytes and slow solution exchange rates, leading to an artificially large potentiation of the peak current in dFBr. This study utilized cell lines with a relatively small surface area and a high-speed perfusion system to achieve fast solution exchange rates, and found the potentiation of the peak current by dFBr to be ~ 1.5 -fold. Further studies involving PAMs of $\alpha 4\beta 2$ nAChRs should take necessary steps to optimize solution exchange rates to improve accuracy and reproducibility of their results.

In addition, analysis of the whole-cell responses of $\alpha 4\beta 2$ nAChRs to dFBr and ACh have lead to new insights on their effect on not only the peak amplitude, but also on the time-to

peak, and the steady-state current. On average, we found that dFBr decreased the time-to peak by 38% and increased the steady-state current ~1.5-fold. Further studies should also consider modulation of the steady-state current to be just as, if not more important than the peak amplitude, as this feature may be a better predictor of the therapeutic benefit of PAMs of $\alpha 4\beta 2$ nAChRs.

Table of Contents

	Page
Signature Page.....	i
Title Page.....	iii
Abstract.....	v
Table of Contents	vii
List of Figures.....	xi
List of Tables.....	xiii
Acknowledgments	xv
Chapter 1: Introduction.....	1
1.1 Summary and Overall Project Aim	1
1.2 Types of Receptor Subunits.....	2
1.3 Functional Properties of Ligand-Gated Ion Channels	3
1.4 The Effects of nAChR Activation on Circuits	3
1.5 The Problem of Receptor Desensitization for Drug Design.....	4
1.6 Positive Allosteric Modulators of $\alpha 4\beta 2$ nAChRs	5
1.7 Electrophysiology Methods: Voltage Clamping	6
Chapter 2: Hypothesis	9
2.1 Nicotinic Receptors Have a High Probability of Opening	9
2.2 Small Cell Size and Fast Solution Exchange Promotes Synchronous Activation of nAChRs	9

2.3 Activation of Silent Receptors.....	11
2.4 Whole-Cell Simulation Models Can Be Compared with Experimental Results.....	11
Chapter 3: Materials and Methods	13
3.1 Cell Culture	13
3.2 Transfection.....	13
3.3 Electrophysiology.....	14
3.4 Whole-Cell Analysis	15
Chapter 4: Results.....	17
4.1 Controls	17
4.1.1 Speed of Perfusion System.....	17
4.1.2 Contamination	17
4.1.3 Voltage Dependent Channel Block	18
4.2 Whole-Cell Data Analysis.....	18
4.2.1 Effects of dFBr on the Time to Peak Current.....	19
4.2.2 Effects of dFBr on the Peak Current	20
4.2.3 Effects of dFBr on the Steady-State Current.....	24
Chapter 5: Discussion.....	29
5.1 The Importance of Fast Application.....	29
5.2 The Importance of Cell Selection.....	30
5.3 Potentiation of the Peak Current.....	30
5.4 Effects of dFBr on Nicotinic Receptor Activation.....	31
5.5 Effects of dFBr on Desensitization.....	31
5.6 dFBr Modulates $\alpha 4\beta 2$ nAChRs in a Stoichiometric-Dependent Manner.....	32

5.7 Defining Modulation	33
Chapter 6: Conclusion	35
Works Cited.....	37

List of Figures

	Page
Figure 1: Perfusion Speed.....	17
Figure 2: Potentiation of the Peak Current by dFBr.....	20
Figure 3: LS Simulation Model.....	21
Figure 4: HS Simulation Model.....	22
Figure 5: LS + HS Simulation Model	22
Figure 6: Potentiation of the Steady-State Current by dFBr.....	24
Figure 7: Normalization of the Peak Current.....	26
Figure 8: Normalization of the Peak Current (LS Simulation).....	26
Figure 9: Normalization of the Peak Current (HS Simulation).....	27
Figure 10: Normalization of the Peak Current (LS + HS Simulation).....	27

List of Tables

	Page
Table 1: Percent Change of 10-90 Rise Times in dFBr.....	19
Table 2: Fold Change of the Peak Current in dFBr.....	23
Table 3: Fold Change of the Steady-State Current in dFBr.....	25

Acknowledgments

I have a tremendous debt of gratitude for all of those who have contributed in any degree to assisting me in this project. In the end, I get to take the credit, but it, in reality, is simply an assimilation of efforts from my mentors, colleagues, professors, friends, and family.

I would like to thank Brian Edmonds for his guidance and mentorship throughout my research. He trusted me throughout this process to find my own path, and to offer assistance when my skillset was not up to par. His insight into the field of nicotinic receptors and how they function was the backbone to this project, not to mention his comments and corrections that he offered for my written thesis.

Brian Edmonds and Arianna Demmerly at the University of Alaska Fairbanks, who provided me with whole-cell simulation models generated from their single-channel data. This viewpoint was extremely valuable in the analysis of my data. By comparing their models to my data, I was able view my data with a unique perspective that shed light on several questions that came up during the analysis process.

I would also like to thank Megan Weltzin at the University of Arizona, for supplying our lab with SH-EP1 cells, stably transfected with $\alpha 4\beta 2$ nicotinic acetylcholine receptors. This contribution made it possible to gather a larger quantity of data than I would have been able to gather otherwise within my given time-frame.

Last, but not least, I would like to thank my wife, Holly, for her support throughout this entire process, for her encouragement that pushed me to finish my project, and for all of the late nights she spent listening to all of my research ideas that were probably less-than interesting.

Chapter 1: Introduction

1.1 Summary and Overall Project Aim

Nicotinic acetylcholine receptors belong to a family of ligand-gated ion channels that mediate synaptic transmission in the central nervous system. nAChRs are proteins composed of five subunits that span the plasma membrane and assemble in the form of a rosette with a central, water-filled pore (Gotti et al., 2009). In response to release of acetylcholine (ACh) from a presynaptic neuron, nAChRs, located on a (downstream) postsynaptic neuron, bind ACh and undergo conformational changes that result in the opening of the central pore. Influx of monovalent and divalent cations through the pore generates an electrical signal that modulates the firing pattern of the postsynaptic neuron (Gay & Yakel, 2007; Williams, Wang, & Papke, 2011).

The functional roles of nAChRs in the CNS are not well defined; however, errors in signaling at cholinergic synapses due to inappropriate expression of nAChRs are associated with cognitive deficits (Perry et al., 2001), nicotine addiction (Xiao et al., 2009), and a variety of catastrophic diseases including Alzheimer's and Parkinson's disease (Court et al., 2001; Perry et al., 1987). A novel class of drugs called positive allosteric modulators (PAMs) targets nAChRs and changes their responses to the binding of acetylcholine. Compounds that enhance or potentiate responses of nAChRs could potentially boost transmission at synapses where nAChRs are underexpressed (deficient) and thereby restore the functional properties of underlying circuits (Williams et al., 2011).

Desformylflustrabromine (dFBr) is a PAM of a subtype of nAChRs that are composed of $\alpha 4$ and $\beta 2$ subunits (Weltzin & Schulte, 2010; Kim et al., 2007). The effects of dFBr on

activation of $\alpha 4\beta 2$ nAChRs has so far been limited to studies of receptors expressed in oocytes. Solution exchange times are slow for the oocyte preparation (Weltzin & Schulte, 2010) relative to the activation time of $\alpha 4\beta 2$ nAChRs (~10 ms) (Grupe, Jensen, Ahring, Christensen, & Grunnet, 2013; Paradiso & Steinbach, 2003), which limits the information that can be obtained concerning the mechanism of action of dFBr on $\alpha 4\beta 2$ nAChRs. The overall aim of this study was to investigate the properties of dFBr on $\alpha 4\beta 2$ nAChRs expressed in SH-EP1 cells using fast, step increases in ACh concentration (concentration jumps). Using a novel apparatus that allowed for fast changes in ACh concentration, we were able to characterize the effect of dFBr on nAChR responses characteristic of receptors *in vivo*.

1.2 Types of Receptor Subunits

The types of subunits, and the order in which they are arranged, determines how nAChRs interact with ACh and other chemical compounds such as agonists and allosteric modulators. Neuronal nAChRs are composed of α ($\alpha 2$ - $\alpha 10$) and β ($\beta 2$ - $\beta 4$) subunits, which form homomeric and heteromeric receptors (Gotti, Zoli, & Clementi, 2006). The major class of nAChRs in the brain is composed $\alpha 4$ and $\beta 2$ subunits that can assemble in alternate receptor stoichiometries (Nelson, Kuryatov, Choi, Zhou, & Lindstrom, 2003). Low sensitivity $\alpha 4\beta 2$ nAChRs (LS) are composed of three $\alpha 4$ subunits and two $\beta 2$ subunits, whereas high sensitivity $\alpha 4\beta 2$ nAChRs (HS) are composed of three $\beta 2$ subunits and two $\alpha 4$ subunits (Carbone, Moroni, Groot-Kormelink, & Bermudez, 2009; Moroni, Zwart, Sher, Cassels, & Bermudez, 2006; Mazzaferro et al., 2014; Kuryatov, Onskan, & Lindstrom, 2008). These differences in stoichiometry have a significant effect on single-channel conductance (Nelson et al., 2003; Li & Steinbach, 2010) and sensitivity to agonists, partial agonists, and antagonists (Carbone et al., 2009; Moroni et al.,

2006; Mazzaferro et al., 2014; Kuryatov et al., 2008). Activation of HS receptors requires the binding of two ACh molecules, one at each of the $\alpha 4/\beta 2$ interfaces. Recent studies suggest that activation of a third ACh binding site on the $\alpha 4/\alpha 4$ interface is also required for full activation of LS receptors (Harpsoe et al., 2011; Mazzaferro et al., 2011).

1.3 Functional Properties of Ligand-Gated Ion Channels

Essential to the signaling role of ligand-gated ion channels is their ability to transition from closed to open conformational states in response to ligand binding. At typical resting membrane potentials, binding of ACh (released from presynaptic neurons) results in sodium ion influx through open nAChRs, depolarizing the postsynaptic membrane. Following termination of the release process, the concentration of ACh at receptors decreases, primarily due to the activity of acetylcholinesterase (AChE), and the probability of nAChRs returning to a closed state (available for activation) increases (Williams et al., 2011). If exposure to an agonist is prolonged, as is expected if AChE inhibitors are present, or exogenous agonists (nicotine, *e.g.*) are used, nAChRs enter long-lived closed, or “desensitized” states, in which ligand binding no longer results in channel opening (Paradiso & Steinbach, 2003).

1.4 The Effects of nAChR Activation on Circuits

nAChRs are found throughout the central nervous system and act primarily by modulating the activity of other neurotransmitter-releasing neurons (Dani & Bertrand, 2009; Gotti et al., 2009). Dysfunction of nAChRs is implicated in several neuronal disorders. The type of dysfunction is dependent on the disease. In patients with Alzheimer’s disease (AD), for example, studies indicate a net decrease in expression of certain nAChR subunits as well as a

decrease in high-affinity nicotine binding sites within the cortex, striatum, and thalamus (Court et al., 2001). Other studies have shown that the cognitive symptoms associated with schizophrenia (Miwa, Freedman, & Lester, 2011) and autism (Lee et al., 2002; Perry et al., 2001) can be associated with a decrease in nAChR expression, while nicotine addiction (Govind, Walsh, & Green, 2012; Xiao et al., 2009) is believed to occur as a result of desensitization that apparently triggers upregulation of $\alpha 4\beta 2$ nAChRs. These and other disorders may be treatable, at least in part, by compounds that increase the activity of nAChRs in an attempt to offset the errors in cholinergic signaling that occur as a result of underexpression or desensitization.

1.5 The Problem of Receptor Desensitization for Drug Design

The rapid desensitization of nAChRs as a result of prolonged exposure to an agonist is a potential obstacle for developing effective treatment options for diseases related to dysfunctional cholinergic signaling. For example, the efficacy of AChE inhibitors used in the treatment of Alzheimer's disease (AD) has been questioned (Birks, 2006), perhaps because these drugs do little to prevent desensitization of nAChRs despite their role in maintaining a relatively high concentration of ACh at cholinergic synapses (Quick & Lester, 2002). Moreover, they lack specificity, leading to poor side-effect profiles (Birks, 2006). It is, therefore, imperative that science and medicine look towards developing pharmacologic agents that not only act on specific nAChR subtypes, but also overcome the obstacle of rapid and profound desensitization. These new compounds may be used in place of, or as an adjunct to current treatment modalities.

1.6 Positive Allosteric Modulators of $\alpha 4\beta 2$ nAChRs

PAMs are compounds that bind to allosteric sites on the receptor, leaving the canonical orthosteric sites free and available to bind agonists (Changeux & Edelstein, 2005). PAMs can act by increasing response amplitude, either by increasing the maximum response to a saturating concentration of agonist (all receptors occupied), by decreasing the concentration of ACh required to achieve a half-maximal response, or by increasing the conductance of the ion channels (Pandya & Yakel, 2011b; Changeux & Edelstein, 2005; Williams et al., 2011).

Some commonly used drugs act by an allosteric mechanism. Benzodiazepines and barbiturates, for example, are PAMs of GABA_A receptors. On a molecular level, benzodiazepines increase the frequency of receptor opening, while barbiturates act by increasing the mean receptor open time (Trevor & Way, 2009). Allosteric modulation, however, is not unique to pharmacology. In fact, many endogenous steroid hormones and peptides act as allosteric modulators, and play an integral role in the regulation of receptor activity *in vivo* (Williams et al., 2011; Pandya & Yakel, 2011b). Research involving allosteric modulators of $\alpha 4\beta 2$ nAChRs has shown considerable promise for the treatment of AD (Pandya & Yakel, 2011a) schizophrenia (Timmerman et al., 2012), and nicotine addiction (Liu, 2013).

Desformylflustrabromine is a PAM of $\alpha 4\beta 2$ nAChRs. It is a tryptamine-derived metabolite from the marine bryozoan *Flustra foliacea* (Kim et al., 2007; Peters, Kong, Terlau, & Wright, 2002). When tested on a variety of nAChR subtypes, dFBr was found to potentiate the peak (macroscopic current) responses to ACh up to 3-fold in *Xenopus laevis* oocytes heterologously expressing a mixture of both HS and LS receptors (Sala et al., 2005; Weltzin & Schulte, 2010). Weltzin and Schulte (2010) also demonstrated that dFBr rescues the same

population of nAChRs from desensitization, and proposed that disruption of desensitized states, or stabilization of open states relative to desensitized states is the mechanism by which dFBr potentiates the macroscopic current.

1.7 Electrophysiology Methods: Voltage Clamping

Voltage-clamping is a method that allows one to measure the response of nAChRs and other ligand-gated ion channels via measurements of the current flowing through open, activated channels. In a whole-cell voltage-clamp experiment a single electrode is used to control ion concentrations within the cell, maintain a constant membrane potential, and measure changes in electrical activity of a cell membrane (Hammond, 2008).

Using this technique, one can record the electrical activity across the membrane of a cell, or, in the case of a modified “patch-clamp” method, of a single ion channel. Analysis of single-channel and whole-cell recordings provides insights regarding the mechanism by which a compound alters receptor kinetics. Single-channel data allows one to determine the unitary conductance of the open channel, as well as distributions of channel open times and shut times for a receptor at a particular drug concentration. This information can then be used to construct a plausible model for channel gating and calculate the rate constants that govern the transitions between various, connected states of the receptor (Hammond, 2008). These kinetic models can then be used to simulate whole-cell responses to a range of concentration profiles of agonist to compliment, and add to findings obtained from whole-cell data.

Whole-cell voltage-clamp recordings yield waveforms that represent changes in current passing through the cell membrane, corresponding to shifts in the conformational states of the receptors expressed on the surface of a cell. In the case of nAChRs, the expected response to a

maintained increase in agonist concentration is a transient influx of cations as nAChRs move from a closed, resting state (conformation), to mostly open states, which then enter long-lived, non-conducting desensitized states. Eventually, the whole-cell current reaches a steady-state, in which the open, closed, and desensitized states of all receptors are in equilibrium. The magnitude of the steady-state current will change as the rate constants, which determine the probability of entering and leaving the various conformational states, change due to exposure to compounds such as dFBr which modulate the gating properties of nAChRs (Demmerly & Edmonds, 2015).

Whole-cell data is commonly analyzed by measuring the peak currents generated at multiple agonist concentrations and plotted as a dose-response relation to determine the efficacy (maximum response relative to other agonists) and potency (concentration that yields a half-maximal response) of an agonist. Modifying experimental procedures, such as the addition of an allosteric modulator, provides insight on changes in efficacy and potency under experimental conditions. The steady-state current, which indicates the effect of prolonged exposure to a compound, as is likely to happen *in vivo* (Brody et al., 2006), can be measured with the use of data analysis software such as Igor Pro. In addition, changes in the rate of decay of the peak current provide insight on the effect of a compound on the time course of development of desensitization.

Chapter 2: Hypothesis

2.1 Nicotinic Receptors Have a High Probability of Opening

dFBr has been shown to cause a three-fold potentiation of the peak current in *Xenopus laevis* oocytes heterologously expressing $\alpha 4\beta 2$ nAChRs (Weltzin & Schulte, 2010). The use of oocytes is associated with slow solution exchange times; therefore, potentiation observed in oocytes may not reflect potentiation *in vivo*, where agonist concentration rises rapidly. My experiments were designed to test whether or not this data is reproducible using smaller, mammalian cells, in which faster solution exchange times are possible.

LS receptors have a high probability of opening ($P_{\text{open}} > 0.8$) when agonist concentration is rapidly stepped, or jumped, to a saturating level of ACh or nicotine (Li & Steinbach, 2010; Demmerly & Edmonds, 2015). Based on this finding, one would not expect the potentiation of the peak current by dFBr to be greater than 25% of the control response. I, therefore, hypothesized that previous reports on the potentiating effects of dFBr were overestimated (Weltzin & Schulte, 2010).

2.2 Small Cell Size and Fast Solution Exchange Promotes Synchronous Activation of nAChRs

Cell size may significantly influence the rate at which one can change experimental solutions while voltage clamping. Oocytes have been used in electrophysiology experiments for decades, because of their relatively large size and ease of use in two-electrode voltage-clamping experiments, as well as their ease in maintenance. Smaller cell lines such as HEK-293 cells and SH-EP1 cells have also been used with increased frequency over the last few decades. In whole-cell experiments, simultaneous exposure of the drug solution to the entire population of receptors

on the cell is important due to the fact that nAChRs are known to be extremely fast activating, and can rapidly enter long-lived desensitized states, depending on the pharmacodynamics of the drug of interest (Paradiso & Steinbach, 2003). To observe a true peak response while voltage clamping, receptors must be activated synchronously. The relatively large surface area of oocytes presents a problem for simultaneous exposure of the drug to the entire population of expressed receptors (Baburin, Beyl, & Hering, 2006).

A phenomenon called the “unstirred layer effect” describes how ion transport is affected by surface area (Wilson & Dietschy, 1974). Essentially, the more surface area that a solution must cover, the more resistance the solution encounters, and the longer it takes to exchange solutes at the surface. Receptors that are closer to the (solution) application pipette are activated and desensitized before receptors that are further away, resulting in asynchronous activation of receptors.

Increasing the speed of solution exchange, in addition to choosing a cell with a smaller surface area, will further promote synchronous activation of all surface receptors. The solution exchange times done by Weltzin & Schulte (2010) were measured on the order of seconds, which is far too slow to capture the true peak current in a cell expressing $\alpha 4\beta 2$ nAChRs.

To this point, Baburin et al. (2006) said, “Fast perfusion of oocytes [and other cell types] is [essential] for studies of ligand-gated ion channels. Large bath volumes and slow perfusion rates prevent fast and timed applications of neurotransmitters resulting in apparently slow applications of the channels and substantial receptor desensitization during the chamber perfusion leading to underestimation of the peak current values.”

Therefore, it is not unreasonable to hypothesize that there may actually be a large proportion of desensitized $\alpha 4\beta 2$ nAChRs at the time that the “peak” current is measured in the

oocyte preparation. If an allosteric modulator were to disrupt or destabilize desensitized states, potentiation in oocytes, where the fraction of desensitized receptors at the time of peak current is significant, would be expected to be large relative to potentiation of currents when receptors are activated rapidly (little or no desensitization). The advantage to testing my hypothesis in SH-EP1 cells, as opposed to oocytes, is that SH-EP1 cells have a relatively small surface area, minimizing the unstirred layer effect and facilitating rapid solution exchange.

2.3 Activation of Silent Receptors

An important finding by Li & Steinbach (2010) yields another potential explanation for a three-fold potentiation of the peak current (Weltzin & Schulte, 2010) that deserves consideration. They showed that HEK cells express ~1000 functional $\alpha 4\beta 2$ nAChRs, however, this number is only ~ 7% of the total number of receptors in the membrane as assessed in radioligand binding experiments (Zhang & Steinbach, 2003; Li & Steinbach, 2010). This observation is consistent with the possibility that the majority of surface receptors (93%) are “silent,” or not available for activation, for unknown reasons (Li & Steinbach, 2010; Papke, 2010). This phenomenon has also been observed in oocytes (Fenster, Whitworth, Sheffield, Quick, & Lester, 1999). A large potentiation of the peak current in SH-EP1 cells is not inconsistent with the idea that a portion of the otherwise silent receptors become available for activation in the presence of dFBr.

2.4 Whole-Cell Simulation Models Can Be Compared with Experimental Results

In addition, we felt that a whole-cell approach, by itself, would not provide us with an adequate understanding of how dFBr modulates $\alpha 4\beta 2$ nAChRs. Although the details of the acquisition of single-channel data and its analysis is outside of the scope of this thesis,

concurrent whole-cell and single-channel data analysis was also used to determine the gating properties of individual receptors and how they are modulated by dFBr. If, using these techniques, one can conclude that the entire effect of potentiation can be accounted for by the modulation of gating properties by dFBr, this would decrease the likelihood that the potentiating effects of dFBr could be attributed to the recruitment of silent receptors.

Chapter 3: Materials and Methods

3.1 Cell Culture

Cell media for SH-EP1 cells stably transfected with $\alpha 4\beta 2$ nAChRs consisted of 500 mL Dulbecco's Modified Eagle's Medium (DMEM) (Gibco®, cat# 11965-092) containing 25 mL Fetal Bovine Serum (Hyclone® cat# SH30071.03), 50 mL Heat Inactivated Horse Serum (Gibco®, cat# 26050-088), 5 mL Sodium Pyruvate (Sigma®, cat# P5280-25G), 10 mL L-Glutamine (Sigma®, cat# G8540-25G), 5 mL Penicillin-Streptomycin (Cellgro®, cat# 30-002-CI), and 100 μ L of Amphotericin B (Sigma®, cat# A9528, 10mg/mL). Cells were seeded at a density of approximately 1×10^6 cells/ T-75 cell culture flask and incubated at 37° C in the presence of 5% CO₂, and passaged every 3 days or when cell culture growth reached 90% confluency. 24 hours prior to experiments, SH-EP1 cells were plated on 35 mm culture dishes at a density of 1×10^5 cells/ dish with 3 mL of fresh media.

Freestyle™ human embryonic cells (HEK F-293) were used in a few preliminary experiments. Cells were maintained in suspension with Gibco© Freestyle™ 293 Expression Medium (Invitrogen®) at 37° C in the presence of 8% CO₂. HEK F-293 cells were seeded at a density of 2×10^5 cells/mL and passaged every three days or when cell density exceeded 1.5×10^6 cells/mL.

3.2 Transfection

HEK F-293 Cells were plated on 35 mm dishes at a density of 2×10^5 cells/mL and allowed to adhere to the dish approximately 24 hours prior to transfection. HEK F-293 cells were transiently transfected with 12 μ g of both $\alpha 4$ and $\beta 2$ nicotinic receptor subunit DNA plasmids,

and allowed to incubate in transfection solution at 37° C and 8% CO₂ for 2-2.5 hours. After transfection incubation period, the transfection solution was removed by aspiration and replaced with fresh media. HEK F-293 cells were allowed to incubate for 24 hours at 37° C and 8% CO₂ prior to any electrophysiology experiments.

3.3 Electrophysiology

The extracellular recording solution was composed of deionized water containing (in mM) 142 NaCl, 2.0 CaCl₂, 1.7 MgCl₂, 5.0 Hepes, 10 Glucose, and 5.4 KCl. pH was adjusted to 7.4 with KOH and sterilized via vacuum filtration through a 0.22 micron filter. The pipette solution contained (in mM) 5.4 NaCl, 0.5 CaCl₂, 4.0 MgCl₂, 5.0 Hepes, 142 KCl, and 5.0 EGTA. pH was adjusted to 7.4 with NaOH and sterilized via vacuum filtration through a 0.22 micron filter. Appropriate concentrations of drug and agonist solutions were prepared from 1 M stock solutions of ACh and 10 mM stock solutions of dFBr in deionized water, degassed, and filtered with a 0.22 micron filter prior to experiments.

Pipettes were pulled to a resistance of 4-8 MΩ using a PMP102 micropipette puller (Microdata Instrument Inc.), coated with Sylgard®, and front- and back-filled with pipette solution. Once the pipette was lowered into the 35 mm dish containing external recording solution using a ROE-200 Micromanipulator (Sutter Instruments), the pipette offset was dialed down to zero using an Axopatch 200B patch-clamp amplifier (Molecular Devices). After touching onto a cell, suction was applied until a seal (minimum resistance: 1 GΩ) was achieved. Strong bursts of suction were applied until large transient spikes appeared on the oscilloscope in the Digidata 1440 interface and pClamp 10 acquisition software (Molecular Devices). Adjustments were made to compensate for pipette capacitance (“fast mag” and “fast τ”), whole-

cell capacitance, and series resistance allowing us to correct for voltage drop occurring at the pipette tip (series resistance error). Membrane voltage was held at -80 mV for all experiments except in a control experiment in which we tested the possibility of voltage-dependent channel block contributed our experiments.

Once in a whole-cell configuration, solutions were applied using a fast-application perfusion system (Lee Mini Valves supplied by Automate Scientific with Automate ValveLink8.2 Controller) pressurized at 0.5 psi. A Perfusion Pencil[®] multi-barrel manifold with 250 micron removable tip was placed adjacent to the target cell so that the cell was directly in the solution stream, and viewed under a 40x water immersion objective (Nikon[®] Eclipse).

3.4 Whole-Cell Analysis

Values for peak current, 10-90 rise time, steady-state current, decay time constants, and associated amplitudes of fitted exponentials were determined using the software program Igor Pro, Version 6.05A (©WaveMetrics, Inc.). The desensitization portion of the waveforms were best fit using a double exponential function.

$$\text{Equation 1: } y = y_0 + A_1 \exp\left(\frac{-(x-x_0)}{\tau_1}\right) + A_2 \exp\left(\frac{-(x-x_0)}{\tau_2}\right)$$

Where y is the slope of the curve, y_0 is the starting y value of the curve, A is the fractional amplitude of the component, τ is the time constant for the component, and $x-x_0$ is the change in time. Changes in the average fractional contribution of A_1 and A_2 , and changes in the mean values of τ_1 and τ_2 in 100 μM ACh and 100 μM ACh + 1 μM dFBr were then calculated.

Chapter 4: Results

4.1 Controls

4.1.1 Speed of Perfusion System

Exchange rates between solutions were performed on HEK F-293 cells. Solution chambers were filled with external (High Na^+) and internal (High K^+) solutions. Solution exchanges resulted in changes in membrane current with a 10-90 rise time of approximately 50 ms (Figure 1). The 10-90 rise time is one method used to measure the speed of the response by determining the time it takes to progress from 10% to 90% of the peak current.

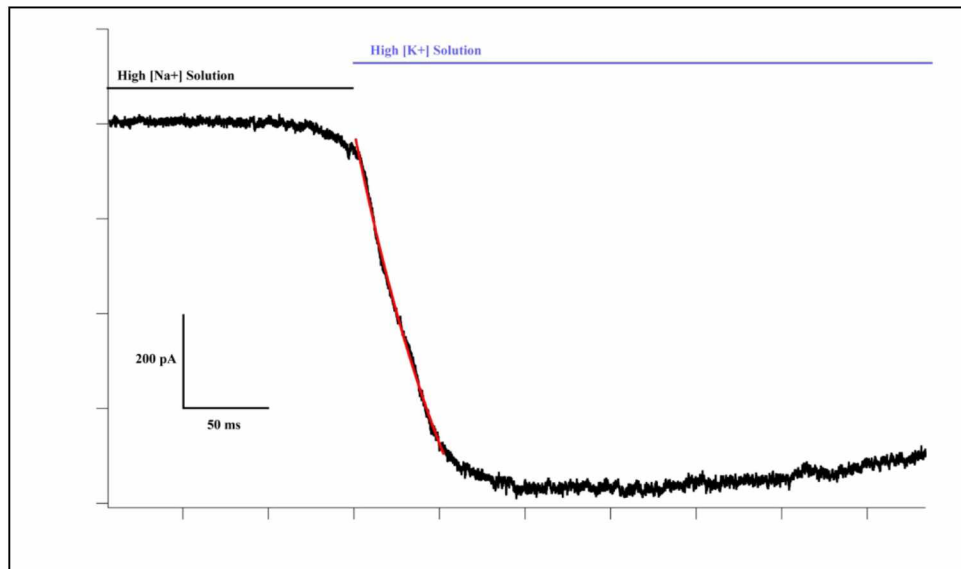


Figure 1: Perfusion Speed. To determine the speed of the perfusion system, external solutions were jumped from high $[\text{Na}^+]$ to high $[\text{K}^+]$, and achieved 10-90 rise times of ~ 50 ms.

4.1.2 Contamination

To test that our recordings were not contaminated by accumulation of drugs in the bath (i.e., drugs outside of the direct solution stream), we performed the following sequence of

solution exchanges: 500 ms control solution, 20 s of 100 (Weltzin & Schulte, 2015) ACh, 2 s control, 2 s 1 μM dFBr. The experiment showed no response when the solution switched to 1 μM dFBr. A positive control was performed using the same outline of solution exchanges replacing 1 μM dFBr with 100 μM ACh + 1 μM dFBr, and a response was observed (data not shown).

4.1.3 Voltage Dependent Channel Block

To explore the possibility of voltage- dependent channel block interfering with experimental results, peak currents were measured using 100 μM ACh and 100 μM ACh + 1 μM dFBr held at a membrane potential of -80 mV and repeated at -30 mV. The difference in fold potentiation between the two sample groups was negligible (1.56-fold and 1.48-fold increase, respectively).

4.2 Whole-Cell Data Analysis

Twenty-one whole-cell recordings (twelve with 100 μM ACh and nine with 100 μM ACh + 1 μM dFBr) performed on SH-EP1 cells were analyzed to examine changes in peak current, 10-90 rise time, steady-state current, and the fraction of the peak current in the steady-state. In addition, similar analyses were performed on whole-cell simulations of HS, LS, and 50% HS + 50% LS receptors using gating models (provided by Demmerly and Edmonds, unpublished) generated from single channel data and were compared alongside the experimental data. Changes in the time constants (refer Equation 1), τ_1 and τ_2 , give insight as to changes in the rate of desensitization. Inconsistent results made it impossible to use this data in a meaningful way.

4.2.1 Effects of dFBr on the Time to Peak Current

The time to peak current differed widely depending on the cell, but I found, in general, that dFBr caused the current to peak more rapidly (Table 1). For example, the 10-90 rise time of Experiment 1 in 100 μM ACh was 238 ms. That same cell in 100 μM ACh + 1 μM dFBr had a 10-90 rise time of 66.5 ms. On average, dFBr yielded a $\sim 38\%$ reduction in the 10-90 rise time, but in two of the four cells, I did not observe a significant change in the 10-90 rise time.

	ACh (ms)	ACh + dFBr (ms)	Percent Change in Rise Time
Experiment 1	238	66.5	-72.0%
Experiment 2	152	41.6	-72.8%
Experiment 3	106	97.9	-7.25%
Experiment 4	65.4	65.8	+0.65%
Average			-37.9%
HS Simulation	25.5	11.1	-56%
LS Simulation	54.0	50.3	-6.85%
HS + LS Simulation	40.5	25.3	-37.5%

In the simulation models, the magnitude of the effect of dFBr on the 10-90 rise time was dependent on the distribution of HS and LS receptors (Table 1). dFBr had the greatest effect on the HS simulation, reducing the 10-90 rise time from ~ 25 ms to ~ 11 ms. The LS simulation yielded a slight reduction in the 10-90 rise time from ~ 54 ms to ~ 50 ms. The HS + LS simulation yielded a reduction in the 10-90 rise time from ~ 41 ms to ~ 25 ms, a $\sim 38\%$ reduction. Also, it is interesting to note the HS simulation reached its peak twice as fast as the LS simulation without dFBr, and about five times as fast with dFBr.

4.2.2 Effects of dFBr on the Peak Current

100 μM ACh produced inward currents in SH-EP1 cells expressing $\alpha 4\beta 2$ nAChRs. The currents peaked rapidly, followed by a decay of the inward current until it reached a steady-state. Co-application of 100 μM ACh with 1 μM dFBr produced inward currents that peaked, on average, with larger amplitudes than currents measured in 100 μM ACh alone (Figure 2).

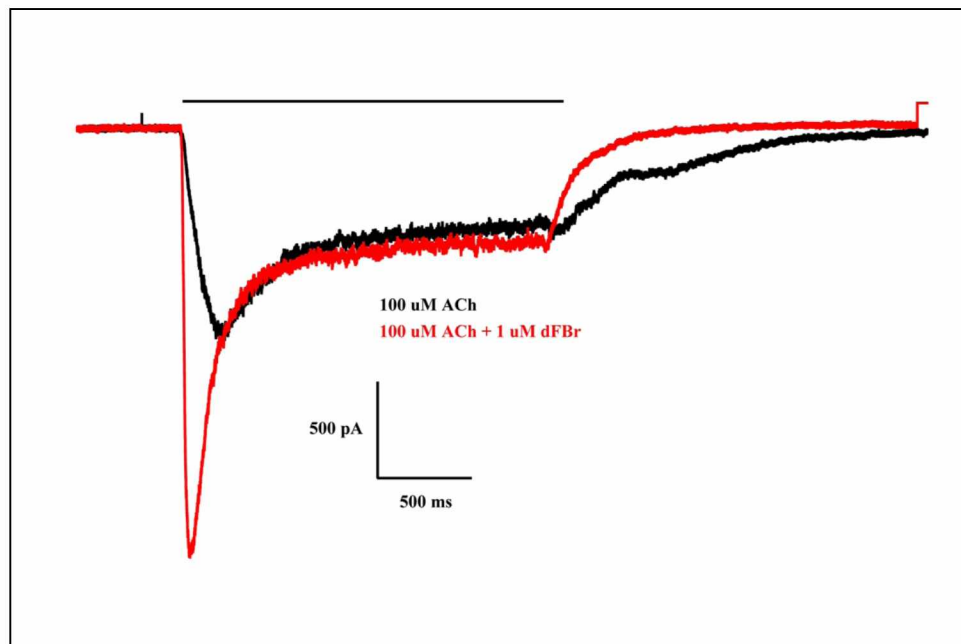


Figure 2: Potentiation of the Peak Current by dFBr. Experimental data (Experiment 2) demonstrating the whole-cell response to 100 μM ACh (black) and 100 μM ACh + dFBr (red). Common among these experiments was the observation that dFBr potentiates the peak current, decreases the time to peak, and changes the steady-state current at which the receptors are in equilibrium. This particular example demonstrated the largest (2-fold) potentiation of all of the recordings.

Consistent with my hypothesis, I observed a 1.57-fold mean increase in the peak current in dFBr (Table 2), which is much lower than what has been previously reported (Weltzin & Schulte, 2010). Potentiation of the peak current ranged from 1.23-fold potentiation to 2-fold potentiation of the peak current.

When a similar analysis was performed on the HS, LS, and HS + LS simulations, the potentiating effects of dFBr on the peak currents increased 1.73-fold, 1.33-fold, and 1.26-fold, respectively (Figures 3, 4, and 5) (Table 2).

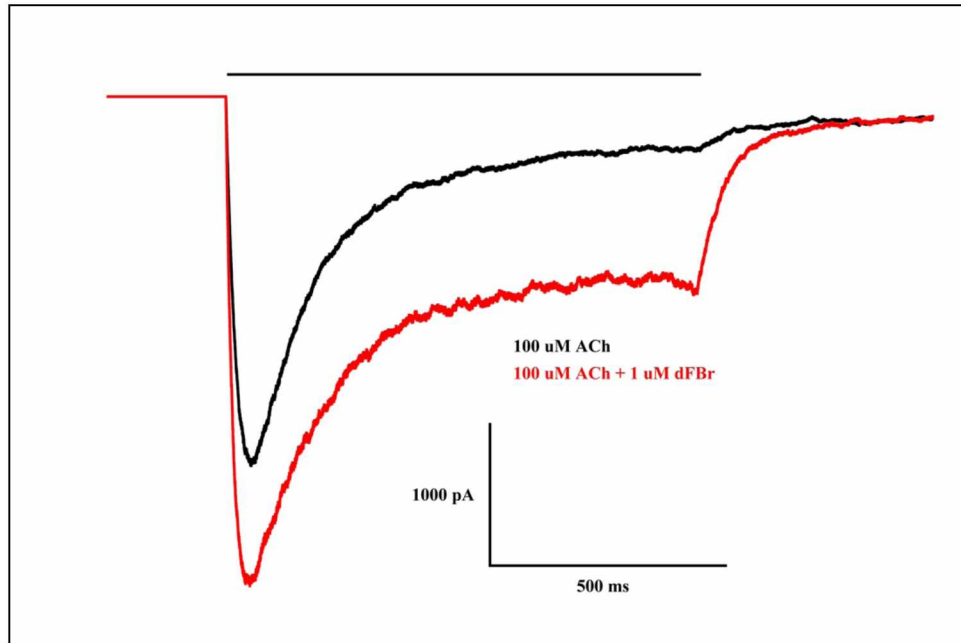


Figure 3: LS Simulation Model. A simulation model demonstrating the theoretical whole-cell response to 100 μ M ACh (black) and 100 μ M ACh + 1 μ M dFBr (red) on a cell expressing only LS receptors.

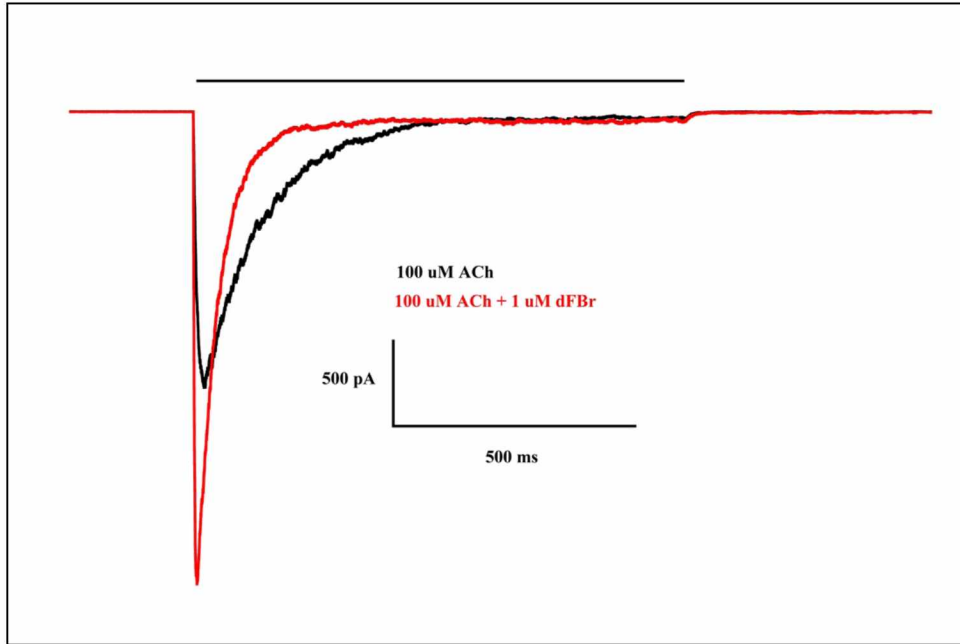


Figure 4: HS Simulation Model. A simulation model demonstrating the theoretical whole-cell response to 100 μM ACh (black) and 100 μM ACh + 1 μM dFBr (red) on a cell expressing only HS receptors.

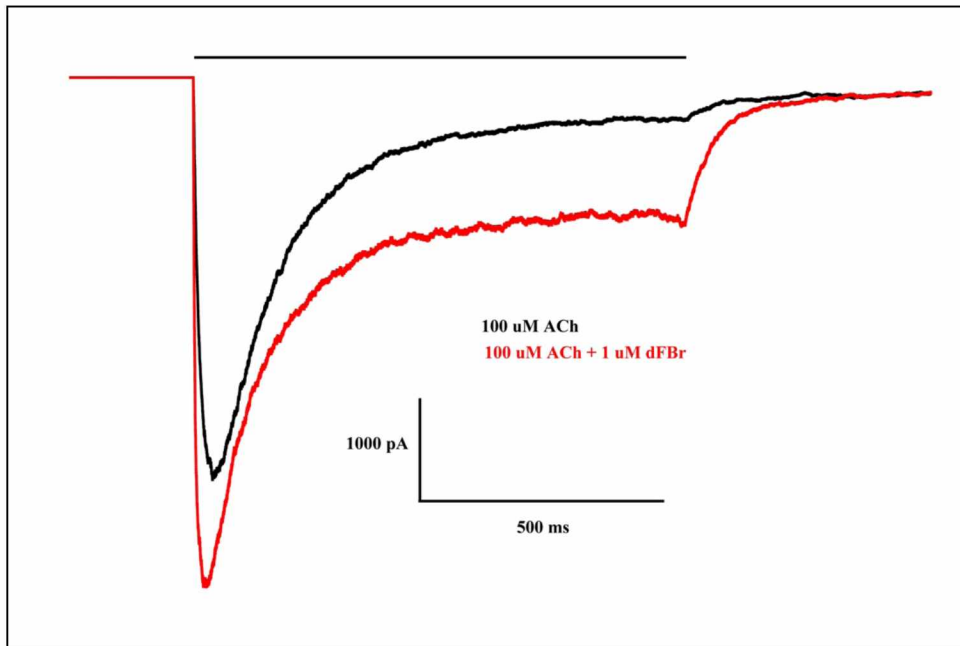


Figure 5: LS + HS Simulation Model. A simulation model demonstrating the theoretical whole-cell response to 100 μM ACh (black) and 100 μM ACh + 1 μM dFBr (red) on a cell expressing an equal ratio of HS and LS receptors.

Table 2: Fold Change of the Peak Current in dFBr			
	ACh (pA)	ACh + dFBr (pA)	Fold Change in dFBr
Experiment 1	-1740	-2430	+1.40
Experiment 2	-1110	-2230	+2.01
Experiment 3	-3461	-4263	+1.23
Experiment 4	-774	-1278	+1.65
Average			+1.57
HS Simulation	-1534	-2651	+1.73
LS Simulation	-2551	-3391	+1.33
HS + LS Simulation	-3859	-4861	+1.26
HS Simulation *	-1440	-1760	+1.22
LS Simulation *	-2252	-3182	+1.41
HS + LS Simulation*	-3678	-4833	+1.31
* These values were taken at a common time point			

One might expect to observe that the potentiation of the peak current of the HS + LS simulation would fall somewhere between the individual HS and LS simulations, however, I found that the potentiation of the peak current in the HS + LS simulation was smaller (+1.26-fold) than both the HS (+1.73-fold) and the LS (+1.33-fold) simulations. In measuring the 10-90 rise times (above), the simulation models indicate that HS and LS receptors activate at different rates. In other words, the peak currents of the three models were occurring at different times. When I measured the current values at the 278 ms time point (the time half-way between the HS dFBr peak and the LS dFBr peak), the potentiation of the current (shown in bold in Table 2) measured in the LS + HS simulation was, in fact, half-way between the values measured for the HS and LS simulations individually. Thus, the peak currents measured in the simulation models were correct.

4.2.3 Effects of dFBr on the Steady-State Current

When the current decays (desensitization) were fit with a double exponential function, the value for y_0 was given and interpreted as the steady-state current value. The experimental data revealed a 1.5-fold increase in the steady-state current with dFBr (Figure 6), similar in magnitude to the HS simulation (1.55-fold increase). The LS simulation, however, showed an even larger (4.20-fold) increase in the steady-state current in dFBr (Table 3). It appears that there was little destabilization of desensitized states at equilibrium in the experimental results in comparison to the LS simulation model. Perhaps the HS:LS expression ratio in SH-EP1 cells is high. This finding was not anticipated in the experimental design, otherwise efforts could have been made to isolate HS and LS nAChRs.

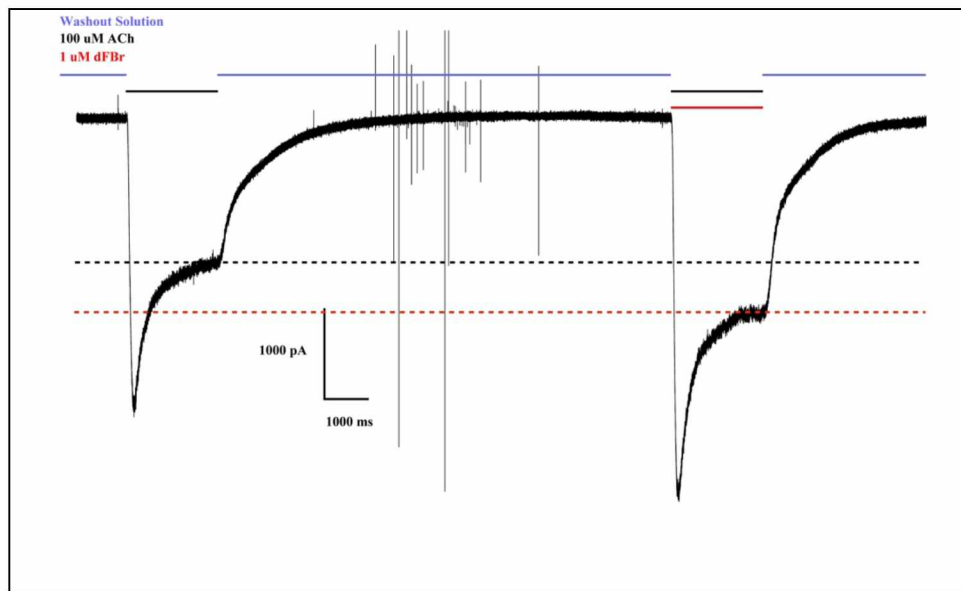


Figure 6: Effect of dFBr on the Steady-State Current. Representative whole-cell recording (Experiment 3) that highlights the effect of dFBr on the steady-state current. The trace on the left was recorded with 100 μM ACh alone. The trace on the right was recorded with 100 μM ACh + 1 μM dFBr. The steady-state currents were estimated with the dashed lines (100 μM ACh in black and 100 μM ACh + 1 μM dFBr in red). Note that the steady-state values in this recording were larger than in other recordings,

but the fold-increase in the steady-state current with dFBr was relatively consistent throughout my experiments.

Table 3: Fold Change of the Steady-State Current in dFBr			
	ACh (pA)	ACh + dFBr (pA)	Fold Change in dFBr
Experiment 1 *	N/A	N/A	N/A
Experiment 2	-428	-645	+1.51 fold
Experiment 3	-1402	-1966	+1.40 fold
Experiment 4	-86.6	-132	+1.53 fold
Average			+1.48 fold
HS Simulation	-33.561	-51.99	+1.55 fold
LS Simulation	-289	-1216	+4.20 fold
HS + LS Simulation	-218	-1288	+5.90 fold
* The appearance of the whole-cell recording made it difficult to confidently determine the steady-state current in this recording.			

To compare waveforms directly, the experimental recordings in 100 μM ACh alone were scaled up so that the peak currents were approximately the same size as the peak currents in 100 μM ACh + 1 μM dFBr (Figure 7). Similar scaling with the simulations were performed and shown in Figures 8, 9 and 10. On gross examination, the desensitizing sag of the experimental data had a similar shape, but with different times to peak (Figure 7). The LS simulation showed a similar time to peak, but the desensitization in dFBr developed more slowly (Figure 8). The HS simulation also showed a similar time to peak, but desensitized more quickly in dFBr (Figure 9). The HS + LS simulation also showed a similar time to peak. Like the LS simulation model, the HS + LS simulation desensitized more slowly in dFBr, but not as slow as the LS simulation (Figure 10).

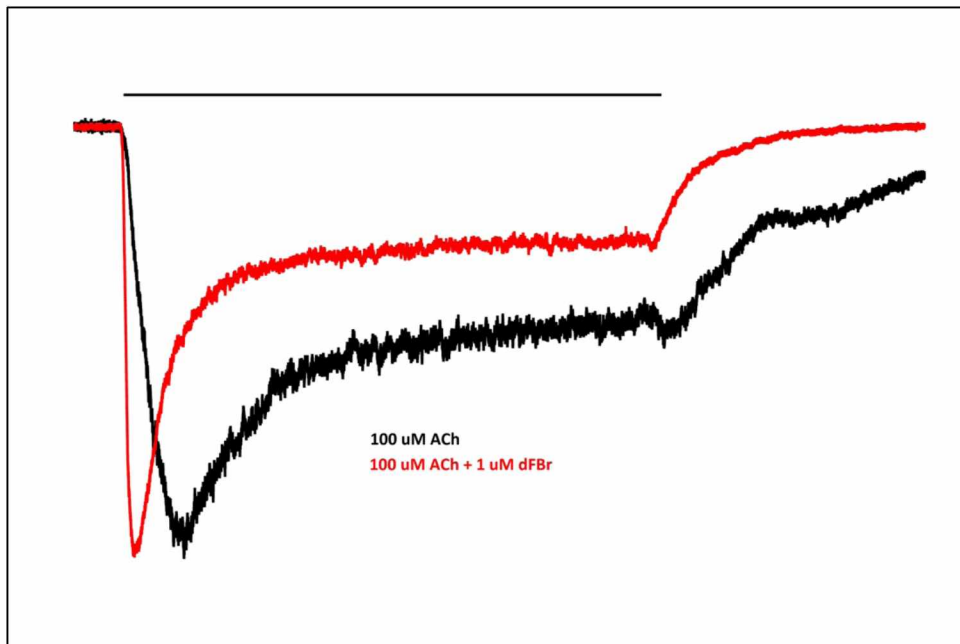


Figure 7: Normalization of the Peak Current. The two traces from Figure 2 were normalized to the peak current to visualize how dFBr affected the general shape of the curve.

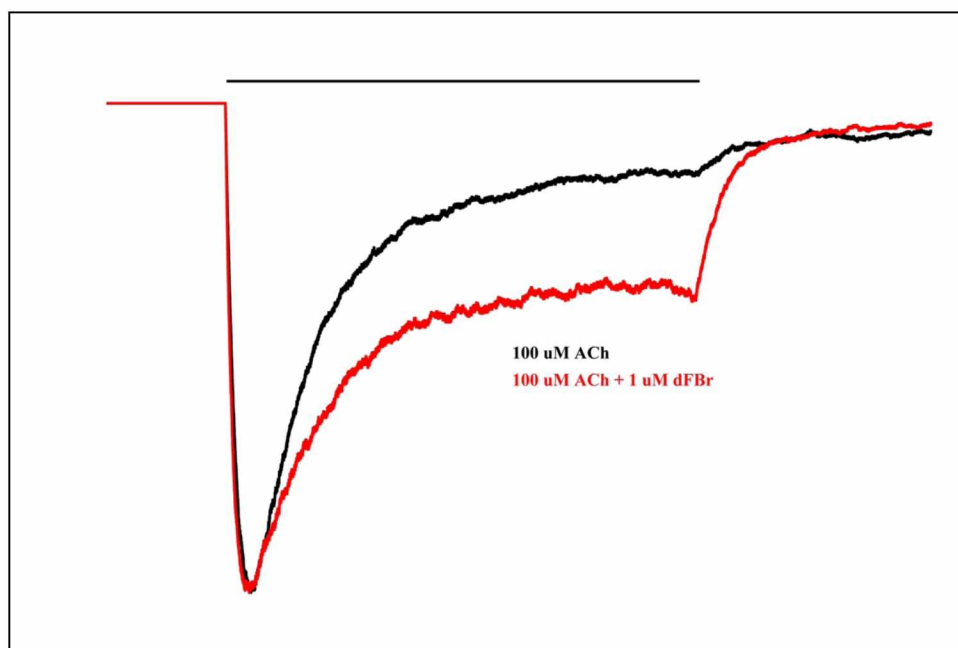


Figure 8: Normalization of the Peak Current (LS Simulation). The two traces from Figure 3 were normalized to the peak current to visualize how dFBr affected the general shape of the curve.

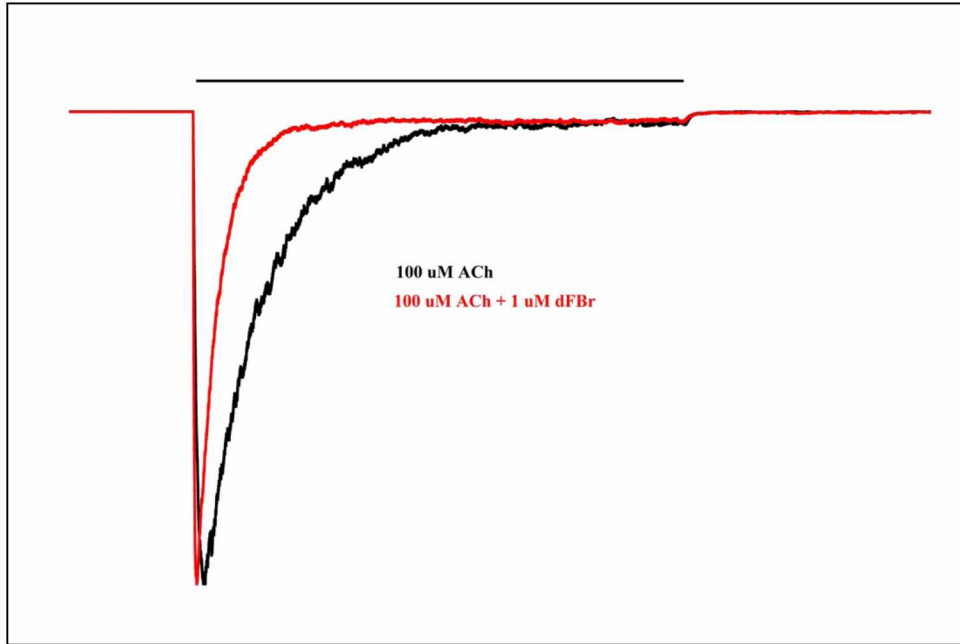


Figure 9: Normalization of the Peak Current (HS Simulation). The two traces from Figure 4 were normalized to the peak current to visualize how dFBr affected the general shape of the curve.

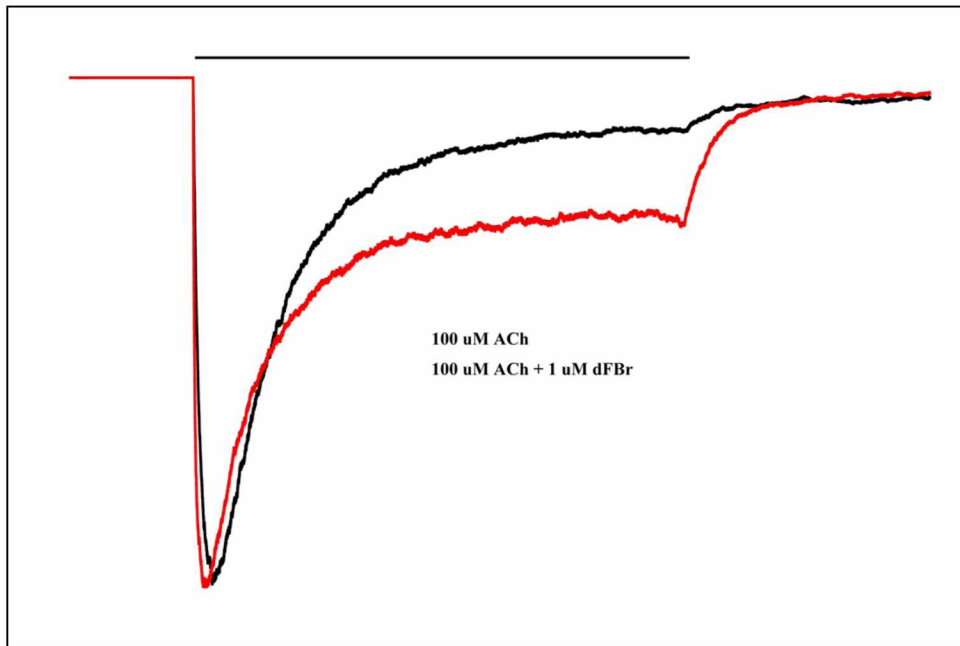


Figure 10: Normalization of the Peak Current (LS + HS Simulation). The two traces from Figure 5 were normalized to the peak current to visualize how dFBr affected the general shape of the curve.

Chapter 5: Discussion

The significance of these findings relate, not only to dFBr and those who study how it modulates $\alpha 4\beta 2$ nAChRs, but to all who utilize patch-clamping methods to study ligand-gating ion channels and other fast-activating ion channels. The importance of synchronous activation of all receptors is emphasized by this study. This principle is fundamental for accuracy and reproducibility, yet it is, unfortunately, commonly overlooked.

Significant findings include a ~ 1.5 -fold potentiation of the peak current, ~ 1.5 -fold potentiation of the steady-state current, and a 38% decrease in the 10-90 rise time when cells expressing $\alpha 4\beta 2$ nAChRs were exposed to dFBr. This study also highlights a new perspective on how we might classify whether or not a drug is an allosteric modulator.

5.1 The Importance of Fast Application

I found that rapid solution exchange is crucial for capturing accurate peak currents in whole-cell experiments with fast-activating $\alpha 4\beta 2$ nAChRs. We were able to achieve exchange rates with 10-90 rise times of approximately 50 ms in control experiments. Faster solution exchange rates were possible, however, our system was somewhat limited by the strength of the adherence of the cells to the petri dishes and to the pipette. Increased pressure in the perfusion system would have allowed for faster exchange rates, however, the cells had a tendency to blow away in the solution stream if the pressure was too great. We found that approximately 0.5-0.75 psi to be the optimal pressure in the perfusion system, using a perfusion pencil with a diameter of 250 microns.

5.2 The Importance of Cell Selection

Cell culture and the selection of a cell line was an ongoing issue throughout my experiments. Several attempts were made at using different cell lines. Initially, experiments were performed using HEK-293 transiently transfected with $\alpha 4$ and $\beta 2$ subunit DNA at equal ratios. An abundance of extracellular material and overcrowding of cells made it difficult to obtain quality seals on our whole-cell patches. The next endeavor was with HEK-F293 cells, which grew in a continuously-agitated solution. HEK-F293 cells had considerably less extracellular debris when plated, but lacked adequate adherence to the plates to allow for fast solution exchange. Finally, stably transfected SH-EP1 cells were used to acquire all of my experimental data, but it also was not without challenges. At times, extracellular debris also made it extremely difficult to obtain quality seals. Time and resources prevented the use of stably-transfected HEK-293 cells, which would have likely been more ideal for my experiments, considering that the ratio of LS to HS nAChRs has been previously determined in this cell type.

5.3 Potentiation of the Peak Current

On average, I observed a 1.57-fold increase in the peak current with dFBr, consistent with my hypothesis that previous reports (Weltzin & Schulte, 2010) were too high. Whole-cell simulation models for LS and HS receptors were similar to my experimental results, +1.33-fold and +1.73-fold, respectively, further supporting my hypothesis. The consistency of my experimental data with the simulation models also argues against the possibility that a 3-fold potentiation could be attributed to the recruitment of silent receptors by dFBr. More likely, these data suggest that the unstirred-layer effect has a greater impact on whole-cell experiments involving $\alpha 4\beta 2$ nAChRs (and likely other types of fast-activating receptors) than has been

realized in the past. Neglecting to minimize the unstirred layer effect by selecting small cell lines and optimizing perfusion speed can result in inaccuracies in the literature.

5.4 Effects of dFBr on Nicotinic Receptor Activation

dFBr decreased the 10-90 rise times in half of my experiments and in the HS simulation, while the 10-90 rise times in the other half of my experiments and the LS simulations were largely unaffected by dFBr. There are many variables that could have lead to this discrepancy. One may speculate that the ratio of LS to HS receptors expressed in individual SH-EP1 cells is not constant. Minute variations in temperature, cell culture, the integrity of the cell membrane, and/or allosteric interactions with other media reagents such as HEPES (Weltzin, Huang, & Schulte, 2014) could have significant impacts on gene expression, post-translational modifications, and dynamics of receptors. Also, variations in cell size and perfusion speed of the experimental solutions could cause mixed-results.

5.5 Effects of dFBr on Desensitization

On average, dFBr caused a ~1.5-fold increase in the steady-state current in my experimental results. In other words, there was more current passing through the membrane at equilibrium in the presence of dFBr. I think this finding is even more significant than the effect of dFBr on the peak current, because the steady-state current represents the (relatively) long-term, rather than transient effects of dFBr on $\alpha 4\beta 2$ nAChRs. This result further reinforces the argument that dFBr and other PAMs of $\alpha 4\beta 2$ nAChRs could be more effective at treating cognitive disorders that result from decreased neuronal cholinergic activity, or augment current treatments. Interestingly, the effect of dFBr on the steady current in the simulation models was

far more pronounced in the LS simulation than in the HS simulation. This may also be a very significant finding, considering that LS receptors make up approximately 80% of neuronal $\alpha 4\beta 2$ nAChRs (Nelson et al., 2003).

5.6 dFBr Modulates $\alpha 4\beta 2$ nAChRs in a Stoichiometric-Dependent Manner

In the simulation models, the effect of dFBr was strikingly dependent on stoichiometry. There was a much larger (4.20-fold) increase in the steady-state current in the LS simulation, and there was barely any steady-state current observed in the HS simulation with or without dFBr. Although dFBr had a greater effect on the peak current in the HS simulation as compared to the LS simulation, the models showed that the current in the HS simulation reached the steady-state more rapidly in dFBr, inferring that dFBr increases the rate at which HS receptors enter one or more desensitized states, or decreases the rate at which they leave those states. The opposite effect was seen in the LS simulation. It took longer for the whole-cell response in the LS simulation to reach the steady-state in the presence of dFBr, and the current was significantly larger.

When the simulations were compared to the experimental data, it appeared as if there was a mixture of HS and LS nAChRs expressed in SH-EP1 cells. The average potentiation of the peak current by dFBr in the experimental results was approximately half-way between the potentiation seen in the HS and LS models.

I observed a significant steady-state current in all of my experimental results that was even more pronounced in dFBr, much like the LS simulation. However, the peak currents in my experimental results desensitized more quickly in the presence of dFBr, much like the HS simulation. Because of these mixed-results, I can only assume that there was a mixture of HS and

LS receptors expressed in the experimental cells, but I am unable to quantify their relative distribution based on these observations alone. In order to make any definitive claims, one would need to isolate the receptor subtypes by using stoichiometry-specific agonists, concatenated receptors, or by adjusting the ratio of subunit DNA during transfection. It is also possible that the gating properties of $\alpha 4\beta 2$ nAChRs are effected by the type of plasma membrane in which these receptors are expressed (HEK cells vs. SH-EP1 cells vs. oocytes, etc.).

5.7 Defining Modulation

Plotting a dose-response curve based on the peak currents measured under different concentration profiles is the standard for determining the modulating-effect of a drug. When a positive change in the peak current is measured, that drug is labeled as a PAM. Although important, my research has taught me that this is a somewhat narrow approach to defining modulation, because it only takes the peak current into account and neglects everything that follows the peak current, namely desensitization and the steady-state current. Because the peak current can be extremely transient and rapidly desensitized, I would encourage future research involving dFBr and other PAMs of $\alpha 4\beta 2$ nAChRs to not neglect its effects on the steady-state current. Its effect on the steady-state in my experimental results and the simulation models is why I believe that dFBr has great potential as a therapeutic agent for the treatment of the cognitive disease mentioned previously. This information would be especially useful if dFBr or other PAMs of $\alpha 4\beta 2$ nAChRs were studied in connection with AChEIs, where the effects of desensitization may be greatest due to prolonged exposure to ACh.

Chapter 6: Conclusion

From these experiments, I am able to conclude that my hypothesis was correct; that optimizing fast solution exchange times made a difference in the observed modulating effects of dFBr, and that slow solution exchange yields an inappropriately high fraction of desensitized nAChRs at the peak. Therefore, when the requirement (for a useful drug) is to alter peak currents, the potential utility of compounds that act by modulating desensitized receptors will be overestimated. To reduce such errors, future *in vitro* research involving fast-activating receptors, such as $\alpha 4\beta 2$ nAChRs, should be performed in smaller cell lines such as HEK-293 cells or SH-EP1 cells, and optimization of solution exchange times should be a critical part of the experimental design.

I can conclude that dFBr, in fact, potentiates the peak current measured in cells expressing $\alpha 4\beta 2$ nAChRs. The results on the effect of dFBr on the rate of desensitization, however, were mixed. This could be due to variability in the expression ratio of HS and LS nAChRs in SH-EP1 cells. The simulation models indicate that dFBr modulates HS and LS nAChRs differently, which was not known to me prior to performing my experiments otherwise more efforts would have been made to isolate the whole-cell responses for HS and LS receptors to more accurately compare experimental results with the simulations.

Furthermore, I believe that the effects of dFBr on the steady-state current are significant; perhaps even more significant than its effect on the peak current. The increase in the steady-state current points to the fact that dFBr does, in fact, shift the ratio of nondesensitized to desensitized receptors at equilibrium. At the very least, the effect of dFBr on the steady-state current should be included in the discussion and an integral part of the assessment of an allosteric modulator.

Works Cited

- Baburin, I., Beyl, S., & Hering, S. (2006). Automated fast perfusion of *Xenopus* oocytes for drug screening. *Pflügers Archiv - European Journal of Physiology*, 453(1), 117-123.
- Birks, J. S. (2006). Cholinesterase inhibitors for Alzheimer's disease. *Cochrane Database of Systematic Reviews*(1).
- Brody, A. L., Mandelkern, M. A., London, E. D., Olmstead, R. E., Farahi, J., Scheibal, D., . . . Mukhin, A. G. (2006). Cigarette Smoking Saturates Brain $\alpha 4\beta 2$ Nicotinic Acetylcholine Receptors. *Archives of General Psychiatry*, 63(8), 907-914.
- Carbone, A. L., Moroni, M., Groot-Kormelink, P. J., & Bermudez, I. (2009). Pentameric concatenated (alpha4)(2)(beta2)(3) and (alpha4)(3)(beta2)(2) nicotinic acetylcholine receptors: subunit arrangement determines functional expression. *The British Journal of Pharmacology*, 156(6), 970-981.
- Changeux, J., & Edelstein, S. J. (2005). Allosteric Mechanisms of Signal Transduction. *Science*, 308(5727), 1424-1428.
- Court, J., Martin-Ruiz, C., Piggott, M., Spurden, D., Griffiths, M., & Perry, E. (2001). Nicotinic receptor abnormalities in Alzheimer's disease. *Biological Psychiatry*, 49(3), 175-184.
- Dani, J. A., Bertrand, D. (2009). Nicotinic Acetylcholine Receptors and Nicotinic Cholinergic Mechanisms of the Central Nervous System. *Annual Review of Pharmacology and Toxicology*, 47, 699-729
- Demmerly, A., & Edmonds, B. W. (2015). Desformylflustrabromine Potentiates High-Sensitivity $\alpha 4\beta 2$ Receptors by Increasing Channel Opening Rate. *Biophysical Journal*, 108(2), 429a.

- Fenster, C. P., Whitworth, T. L., Sheffield, E. B., Quick, M. W., & Lester, R. A. (1999). Upregulation of Surface $\alpha 4\beta 2$ Nicotinic Receptors is Initiated by Receptor Desensitization After Chronic Exposure to Nicotine. *The Journal of Neuroscience*, *19*(12), 4804-4814.
- Gay, E., & Yakel, J. (2007). Gating of nicotinic ACh receptors; new insights into structural transitions triggered by agonist binding that induce channel opening. *The Journal of Physiology*, *584*(3), 727-733.
- Gotti, C., Clementi, F., Fornari, A., Gaimarri, A., Guiducci, S., Manfredi, I., ... Zoli, M. (2009). Structural and functional diversity of native brain neuronal nicotinic receptors. *Biochemical Pharmacology*, *78*(7), 703-711.
- Gotti, C., Zoli, M., & Clementi, F. (2006). Brain nicotinic acetylcholine receptors: native subtypes and their relevance. *Trends in Pharmacological Sciences*, *9*, 482-491.
- Govind, A., Walsh, H., & Green, W. N. (2012). Nicotine-Induced Upregulation of Native Neuronal Nicotinic Receptors is Caused by Multiple Mechanisms. *The Journal of Neuroscience*, *32*(6), 2227-2238.
- Grupe, M., Jensen, A. A., Ahring, P. K., Christensen, J. K., & Grunnet, M. (2013). Unravelling the mechanism of action of NS9283, a positive allosteric modulator of $(\alpha 4)_3(\beta 2)_2$ nicotinic ACh receptors. *British Journal of Pharmacology*, *168*(8), 2000-2010.
- Hammond, C. (2008). The Voltage-Gated Channels of Na⁺ Action Potentials. In C. Hammond, *Cellular and Molecular Neurophysiology* (Third ed., pp. 45-82). Amsterdam: Elsevier Ltd.
- Harpsoe, K., Ahring, P., Christensen, J., Jensen, M., Peters, D., & Baile, T. (2011). Unraveling the High-and Low-Sensitivity Agonist Responses of Nicotinic Acetylcholine Receptors. *The Journal of Neuroscience*, *31*(30), 10759-10766.

- Kim, J. S., Pandya, A., Weltzin, M., Edmonds, B. W., Schulte, M. K., & Glennon, R. A. (2007). Synthesis of desformylflustrabromine and its evaluation as an $\alpha 4\beta 2$ and $\alpha 7$ nACh receptor modulator. *Bioorganic & Medicinal Chemistry Letters*, *17*(17), 4855-4860.
- Kuryatov, A., Onskan, J., & Lindstrom, J. (2008). Roles of Accessory Subunits in $\alpha 4\beta 2^*$ Nicotinic Receptors. *Molecular Pharmacology*, *74*(1), 132-142.
- Lee, M., Martin-Ruiz, C., Graham, A., Court, J., Jaros, E., Perry, R., . . . Perry, E. (2002). Nicotinic receptor abnormalities in the cerebellar cortex in autism. *Brain*, *125*(7), 1483-1495.
- Li, P., & Steinbach, J. H. (2010). The neuronal nicotinic $\alpha 4\beta 2$ receptor has a high maximal probability of being open. *British Journal of Pharmacology*, *160*(8), 1906-1915.
- Liu, X. (2013). Positive allosteric modulation of $\alpha 4\beta 2$ nicotinic acetylcholine receptors as a new approach to smoking reduction: evidence from a rat model of nicotine self-administration. *Psychopharmacology*, *230*(2), 203-213.
- Mazzaferro, S., Benallegue, N., Carbone, A., Gasparri, F., Vijayan, R., & Biggin, P. C. (2011). Additional Acetylcholine (ACh) Binding Site at $\alpha 4/\alpha 4$ Interface of $(\alpha 4\beta 2)_2\alpha 4$ Nicotinic Receptor Influences Agonist Sensitivity. *The Journal of Biological Chemistry*, *286*, 31043-31054.
- Mazzaferro, S., Gasparri, F., New, K., Alcaïno, C., Fuandez, M., Vasquez, P. I., . . . Bermudez, I. (2014). Non-equivalent Ligand Selectivity of Agonist Sites in $(\alpha 4\beta 2)_2\alpha 4$ Nicotinic Acetylcholine Receptors. *The Journal of Biological Chemistry*, *289*(31), 21795-21806.
- Miwa, J., Freedman, R., & Lester, H. A. (2011). Neural Systems Governed by Nicotinic Acetylcholine Receptors: Emerging Hypotheses. *Neuron*, *70*(1), 20-33.

- Moroni, M., Zwart, R., Sher, E., Cassels, B. K., & Bermudez, I. (2006). $\alpha 4\beta 2$ Nicotinic Receptors with High and Low Acetylcholine Sensitivity: Pharmacology, Stoichiometry, and Sensitivity to Long-Term Exposure to Nicotine. *Molecular Pharmacology*, 70(2), 755-768.
- Nelson, M. E., Kuryatov, A., Choi, C. H., Zhou, Y., & Lindstrom, J. (2003). Alternate Stoichiometries of $\alpha 4\beta 2$ Nicotinic Acetylcholine Receptors. *Molecular Pharmacology*, 63(2), 332-341.
- Pandya, A., & Yakel, J. L. (2011a). Allosteric Modulator Desformylflustrabromine Relieves the Inhibition of $\alpha 2\beta 2$ and $\alpha 4\beta 2$ Nicotinic Acetylcholine Receptors by β -Amyloid₁₋₄₂ Peptide. *Journal of Molecular Neuroscience*, 45(1), 42-47.
- Pandya, A., & Yakel, J. L. (2011b). Allosteric modulators of the $\alpha 4\beta 2$ subtype of Neuronal Nicotinic Acetylcholine Receptors. *Biochemical Pharmacology*, 82(8), 952-958.
- Papke, R. (2010). $\alpha 4\beta 2$ Nicotinic acetylcholine receptors, willing if able. *British Journal of Pharmacology*, 160(8), 1903-1905.
- Paradiso, K., & Steinbach, J. H. (2003). Nicotine is highly effective at producing desensitization of rat $\alpha 4\beta 2$ neuronal nicotinic receptors. *The Journal of Physiology*, 553(3), 857-871.
- Perry, E. K., Perry, R. H., Smith, C. J., Dick, D. J., Candy, J. M., Edwardson, J. A., . . . Blessed, G. (1987). Nicotinic receptor abnormalities in Alzheimer's and Parkinson's diseases. *Journal of Neurology, Neurosurgery, and Psychiatry*, 50, 806-809.
- Perry, W. K., Lee, M. L., Martin-Ruiz, C. M., Court, J. A., Volsen, S. G., Merrit, J., . . . Wenk, G. L. (2001). Cholinergic Activity in Autism: Abnormalities in the Cerebral Cortex and Basal Forebrain. *The American Journal of Psychiatry*, 158(7), 1058-1066.

- Peters, L., Kong, G. M., Terlau, H., & Wright, A. D. (2002). Four New Bromotryptamine Derivatives from the Marine Bryozoan *Flustra foliacea*. *Journal of Natural Products*, 65(11), 1633-1637.
- Quick, M. W., & Lester, R. A. (2002). Desensitization of neuronal nicotinic receptors. *Journal of Neurobiology*, 53(4), 457-478.
- Sala, F., Mulet, J., Reddy, K., Bernal, J. A., Wikman, P., Valor, L. M., . . . Sala, S. (2005). Potentiation of human $\alpha 4\beta 2$ neuronal nicotinic receptors by a *Flustra foliacea* metabolite. *Neuroscience Letters*, 373(2), 144-149.
- Timmerman, D. B., Sandager-Nielsen, K., Dyhring, T., Smith, M., Jacobsen, A.-M., Nielsen, E. Ø., . . . Ahring, P. K. (2012). Augmentation of cognitive function by NS9283, a stoichiometry-dependent positive allosteric modulator of $\alpha 2$ - and $\alpha 4$ -containing nicotinic acetylcholine receptors. *British Journal of Pharmacology*, 167(1), 164-182.
- Trevor, A. J., & Way, W. L. (2009). Sedative-Hypnotic Drugs. In B. G. Katzung, S. B. Masters, & A. J. Trevor, *Basic and Clinical Pharmacology* (11 ed., pp. 371-386). New York: McGraw Hill Medical.
- Weltzin, M. M., & Schulte, M. K. (2010). Pharmacological Characterization of the Allosteric Modulator Desformylflustrabromine and Its Interaction with $\alpha 4\beta 2$ Neuronal Nicotinic Acetylcholine Receptor Orthosteric Ligands. *The Journal of Pharmacology and Experimental Therapeutics*, 334(3), 917-926.
- Weltzin, M. M., & Schulte, M. K. (2015). Desformylflustrabromine Modulates $\alpha 4\beta 2$ Neuronal Nicotinic Acetylcholine Receptor High- and Low-Sensitivity Isoforms at Allosteric Clefts Containing the $\beta 2$ Subunit. *The Journal of Pharmacology and Experimental Therapeutics*, 354(2), 184-194.

- Weltzin, M., Huang, Y., & Schulte, M. (2014). Allosteric modulation of alpha4beta2 nicotinic acetylcholine receptors by HEPES. *European Journal of Pharmacology*, 732(5), 159-168.
- Williams, D. K., Wang, J., & Papke, R. L. (2011). Positive allosteric modulators as an approach to nicotinic acetylcholine receptor-targeted therapeutics: advantages and limitations. *Biochemical Pharmacology*, 82(8), 915-930.
- Wilson, F. A., & Dietschy, J. M. (1974). The intestinal unstirred layer: Its surface area and effect on active transport kinetics. *Biochimica et Biophysica Acta*, 363(1), 112-126.
- Xiao, C., Nashmi, R., McKinney, S., Cai, H., McIntosh, J. M., & Lester, H. A. (2009). Chronic Nicotine Selectively Enhances $\alpha 4\beta 2^*$ Nicotinic Acetylcholine Receptors in the Nigrostriatal Dopamine Pathway. *The Journal of Neuroscience*, 29(40), 12428-12439.
- Zhang, J., & Steinbach, J. H. (2003). Cytisine binds with similar affinity to nicotinic $\alpha 4\beta 2$ receptors on the cell surface and in homogenates. *Brain Research*, 959(1), 98-102.